



Thu Dau Mot University
Journal of Science

ISSN 2615 - 9635

journal homepage: ejs.tdmu.edu.vn



A DFT study of the adsorption of F atoms on germanene nanoribbons

by *Vo Van On, Nguyen Duy Khanh, Nguyen Thanh Tung, Hoang Van Ngoc and Huynh Thi Phuong Thuy (Thu Dau Mot University)*

Article Info: Received July 13th, 2022, Accepted Aug. 19th, 2022, Available online Sep. 15th, 2022

Corresponding author: onvv@tdmu.edu.vn

<https://doi.org/10.37550/tdmu.EJS/2022.03.315>

ABSTRACT

In the paper, we investigate the structure and electronic properties of the pristine germanene nanoribbon and four adsorption configurations of 1F and 2F on the substrate of germanene nanoribbon. We obtained the parameters of the most stable structures of pristine germanene nanoribbon and four adsorption configurations. The band structure and the density of state and the part density of state for each element were also obtained. Findings show the adsorption configuration of 1F-GeNR. bridge has no band structure, while other configurations are semimetals with band gap from 0.175eV to 0.67eV; both four adsorption configurations are chemisorption and non-magnetic. The charge distribution of all configurations also was investigated; it showed that there is a charge shift from Ge atoms towards F atoms due to their electronegativity difference.

Keywords: *nanoribbon germanene, fluor adsorption, structure properties, electronic properties*

1. Introduction

Recently, two-dimensional hexagonal lattices such as silicene and germanene have attracted special attention. They have a warped honeycomb structure of sp^3 and sp^2 hybridization in reverse to the planar honeycomb lattice of graphene. Despite this difference, they exhibit some similarities to graphene in electronic and physical

properties and also exhibit semi-metallic nature with no band gap (Balendhran et al., 2015; Cahangirov et al., 2009; Dimoulas et al., 2015). Fabrication of germanene sheets on Pt (111) (Li et al., 2014), Ag(111) (H. Oughaddou et al., 2000), Al(111) (Derivaz et al., 2015), Au (E.Dávila et al., 2014) and Ge₂Pt (Bampoulis et al., 2014) crystals was performed. It has been suggested that silicene and germanene are expected to enhance the performance and scalability of current Si-based nanotechnology (Jiang et al., 2014). Notably, the special mechanical properties of silicene and germanene make them candidates for the design of sensing applications (Balendhran et al., 2015; Anota et al., 2013). Unlike the two-dimensional structure, nano bands can create an electron band gap, and thus they may be promising candidates for next-generation integrated circuit (IC) device components such as transistor channels (Abhinav et al., 2014) and sensors (Bayani et al., 2016). Germanene carbon nanotubes were experimentally synthesized by Han et al. (Han et al., 2005). They exhibit interesting properties similar to those of graphene nanoribbons (Cahangirov et al., 2010; Matthes et al., 2014; Dong et al., 2015). Theoretical studies of electronic properties have established that armchair germanene four nano bands are non-magnetic semiconductors with a direct band gap at the point Γ (Pang et al., 2011). Like graphene, the adsorption of organic and conventional gas molecules on germanene nanostructures has also been reported and its application as a gas sensor has been examined (Rubio-Pereda et al., 2015; Wang et al., 2016; Pang et al., 2017). The atomic binding for germanene is much stronger than for graphene, and the calculated adsorption energy for germanene is higher than that of the molecules adsorbed on graphene and silicene (Xia et al., 2014). Germanene could be a promising candidate in bioelectronics (Chimene et al., 2015). While the adsorption of common gases on 2D germanene sheets and germanene nanostructures has been studied extensively, the adsorption of atoms, especially highly electronegative atoms such as F, on germanene nano bands has not been thoroughly studied. Therefore, our objective is to study the adsorption properties of the F atoms on germanene nanoribbon in this paper. The main objective of this paper is to understand the most stable adsorption configurations, binding energies, densities of states, specific densities of states, and region structures of the system. Furthermore, the charge density redistribution was also studied. The paper is planned as follows: in section 2, the computational method is presented; section 3 presents the adsorption configuration; the adsorption energy in section 4; band structure and density of state in section 5; the charge distribution in section 6; the conclusion of the paper in section 7.

2. Computational Method

The Vienna Ab initio simulation package (VASP) was employed (Kresse et al., 1996) to perform the current density functional theoretical (DFT) calculations. Using the Perdew–

Burke–Ernzerhof (PBE) potential under the frame of generalized gradient approximation (GGA) as the electronic exchange and correlation potential was investigated (Perdew et al., 1996). The convergence criteria of energy and force were 1×10^{-6} eV and 0.01 eV/Å, respectively. The electronic structure calculations were evaluated at the level of GGA-PBE. For plane wave expansion, an energy cutoff of 450 eV was preferred. To sample the k-points in the Brillouin zone, a $1 \times 1 \times 13$ Monkhorst-Pack k-point mesh size was used (Monkhorst et al., 1976). The vacuum spacing of 18 Å perpendicular to the GeNR plane was assumed to avoid the coupling effects between the layers.

3. The adsorption configuration

Pristine germanene nanoribbon consists of 12 atoms of Ge in a zigzag form. It consists of 2 closed strings and a half of an open one. The first point and the endpoint of the nanoribbon are passivized by two hydrogen atoms shown in fig.1. When the F atoms are directly on the bridge between the two closed strings, the configurations are noted as 1F-GeNR.bridge (1b) and 2F-GeNR.bridge (1d), while if the F atoms are not on the bridge, the configurations are noted 1F-GeNR.out (1c) and 2F-GeNR.out (1e). The average bond length between two Ge-Ge atoms is about 2.41 Å to 2.48 Å, as shown in Table 1.

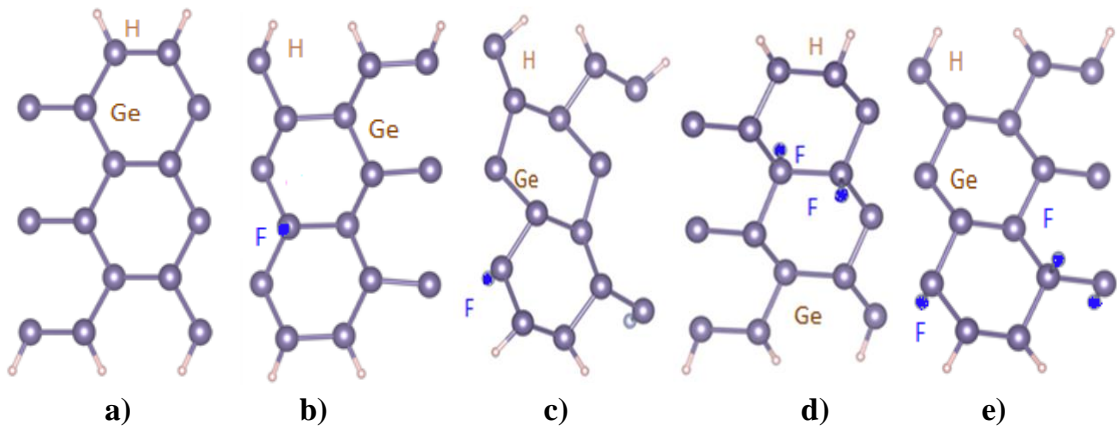


Figure 1. Top view of pristine germanene nanoribbon (a) and adsorption configurations of 1F-GeNR.bridge (b); 1F-GeNR.out(c); 2F-GeNR.bridge (d), and 2F-GeNR.out (e)

TABLE I. Optimal structure parameters and the binding energy

The system	The average bond length(Å)	Minimum distance (F-Ge)(Å)	Binding energy (eV)	Max Buckling(Å)
Pristine GeNR	2.41	no	-60.11	0.64
1F-GeNR.bridge	2.44	1.83	-64.55	1.06
1F-GeNR.out	2.48	1.83	-63.17	0.64
2F-GeNR.bridge	2.45	1.82	-69.63	0.74
2F-GeNR.out	2.45	1.82	-69.50	0.64

Before exploring the electronic properties of germanene nanoribbons when they adsorbed F atoms, we first would like to discuss the most stable structure when they adsorb F atoms. We choose two adsorption types of F atoms on the substrate: F atoms adsorb on Ge atoms at the bridge that connects two closed rings and at the site out the bridge. First, both four sites as a top, hollow, valley, and bridge are chosen when optimizing the adsorption configuration of F-GeNR and 2F-GeNR. The most stable configuration of the four adsorption configurations is one where the F atom is in the top positions as shown in Fig.1. We can see that after the adsorption of F atoms, the bond length between Ge atoms on the substrate increases slightly. Specifically, the maximum bond lengths increased by 2.9% for the configuration of 1F-GeNR.out; the minimum distance between F atom and Ge atom in germanene nano bands is not much different, from 1.82 Å to 1.83 Å. It is also clear that the substrate of the 1F-GeNR adsorption configuration is slightly bent towards the F atom when adsorbing it onto the substrate surface, while the substrate remains flat when adsorbing 2 F atoms at relatively symmetrical positions through the substrate plane. The buckling of the substrate after adsorption also tends to increase due to a force pulling the Ge atom towards the F atom by the large electronegativity difference between the F atom and the Ge atom.

4. The adsorption Energy

To obtain the most stable configuration, we first calculated the adsorption energy (E_{ad}) of considered configurations. The following relation has been used for calculating the E_{ad} : $E_{ad} = E_{total} - E_{substrate} - E_{atom}$ (1)

Where E_{total} , $E_{substrate}$, and E_{atom} are the total energy of the adsorption system, the substrate, and F atoms adsorbed on germanene nanoribbons, respectively. As per the definition adopted here, negative adsorption energy exhibits that the process is exothermic while the magnitude signifies thermodynamic stability. The calculation results showed that the adsorbed samples with the most stable adsorbed energy both are in top positions. The distances from the F atom to the substrates in four configurations are slightly equal and about 1.82 Å to 1.83 Å. Both four adsorption configurations are chemisorption as shown in table 2.

TABLE 2. The adsorption energy of systems

Configuration	Adsorption energy per atom K (eV)	Band gap(eV)
Pristine GeNR	no	0.50
1F-GeNR.bridge	-2.96	no
1F-GeNR.out	-2.4	0.35
2F-GeNR.bridge	-2.07	0.175
2F-GeNR.out	-3.35	0.67

From Table 2, the adsorption energy in the configuration of 2F-GeNR.out is the lowest, and its band structure is largest while the adsorption energy of the configuration of 2F-GeNR.bridge is highest and the band structure is smallest.

5. Band structure and Density of State

Figure 2 shows the band structure and the density of state of the pristine germanene nanoribbon.

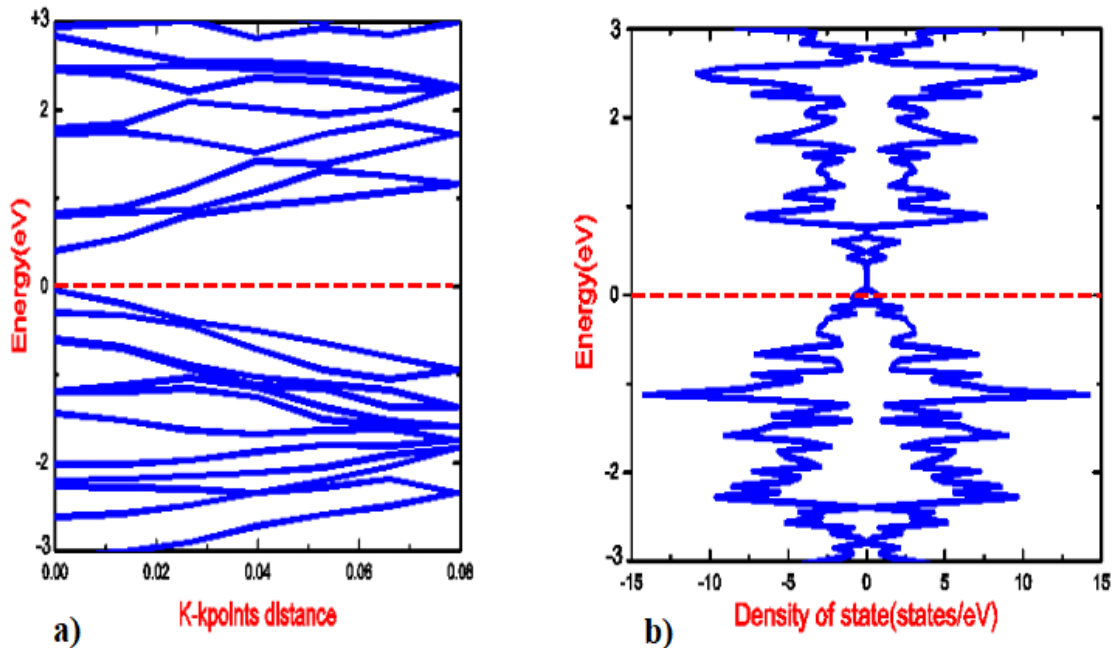


Figure 2. The band structure and the density of state of the pristine germanene nanoribbon

The direct band gap of the pristine nanoribbon germanene is 0.5 eV, it behaves as a semi-metallic property with the electrons predominating, and the Fermi level is closed at the top of the valence region. The electrons mainly concentrate in the valence region with low energy and the conduction region with high energy. In figure 3, the band structure and state density of adsorption configurations of 1F-GeNR.bridge and 2F-GeNR.bridge shown. We can see the adsorption configuration of 1F-GeNR.bridge has no band structure, while that of 2F-GeNR.bridge is 0.175eV, it is a semimetal, and the Fermi level overlaps the bottom of the conductive region. The density of state of the adsorption configuration of 1F-GeNR.bridge concentrates significantly closed to Fermi level, while that of 2F-GeNR.bridge, the electron state densities are mostly slightly farther away in the high energy region. We can see that the graphs of the densities of state of pristine configure and all adsorption configurations are symmetric fully for the x-axis, which shows configures have no magnetization.

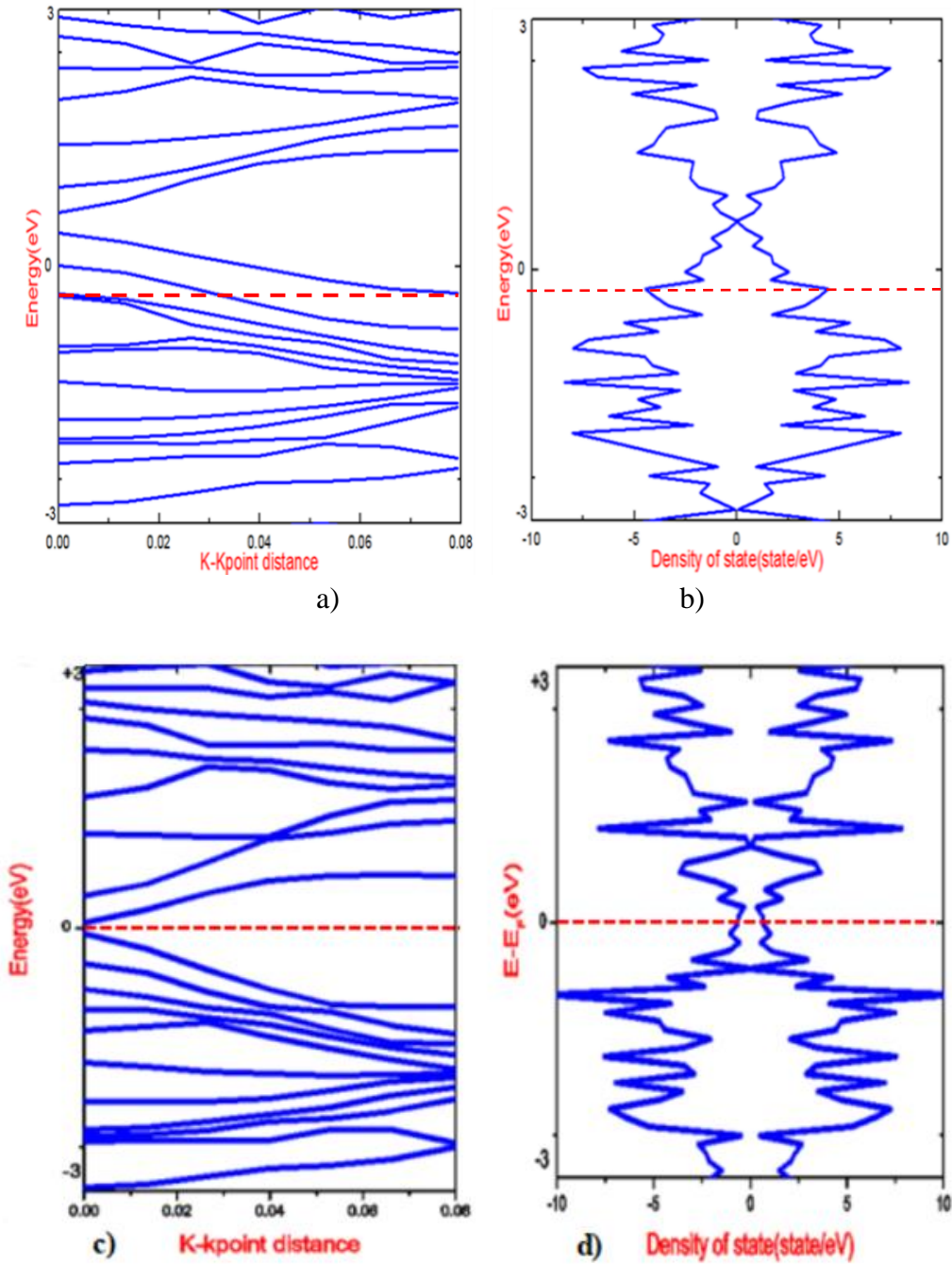


Figure 3. Band structures and the density of state of adsorption configurations of 1F-GeNR.bridge (a, b), and 2F-GeNR.bridge (c, d).

Figure 4 shows the band structure and the density of state of configurations of 1F-GeNR.out, and 2F-GeNR.out. We can see configuration of 1F-GeNR.out is a semimetal with an indirect band gap of about 0.35eV, while that of 2F-GeNR.out is a metal with a direct band gap of 0.67eV. From figure 4 we also see that the electron density of the substrate of 2F-GeNR.out is reduced more than that of 1F-GeNR.out because the electrons are pulled more towards the more electronegative F atoms.

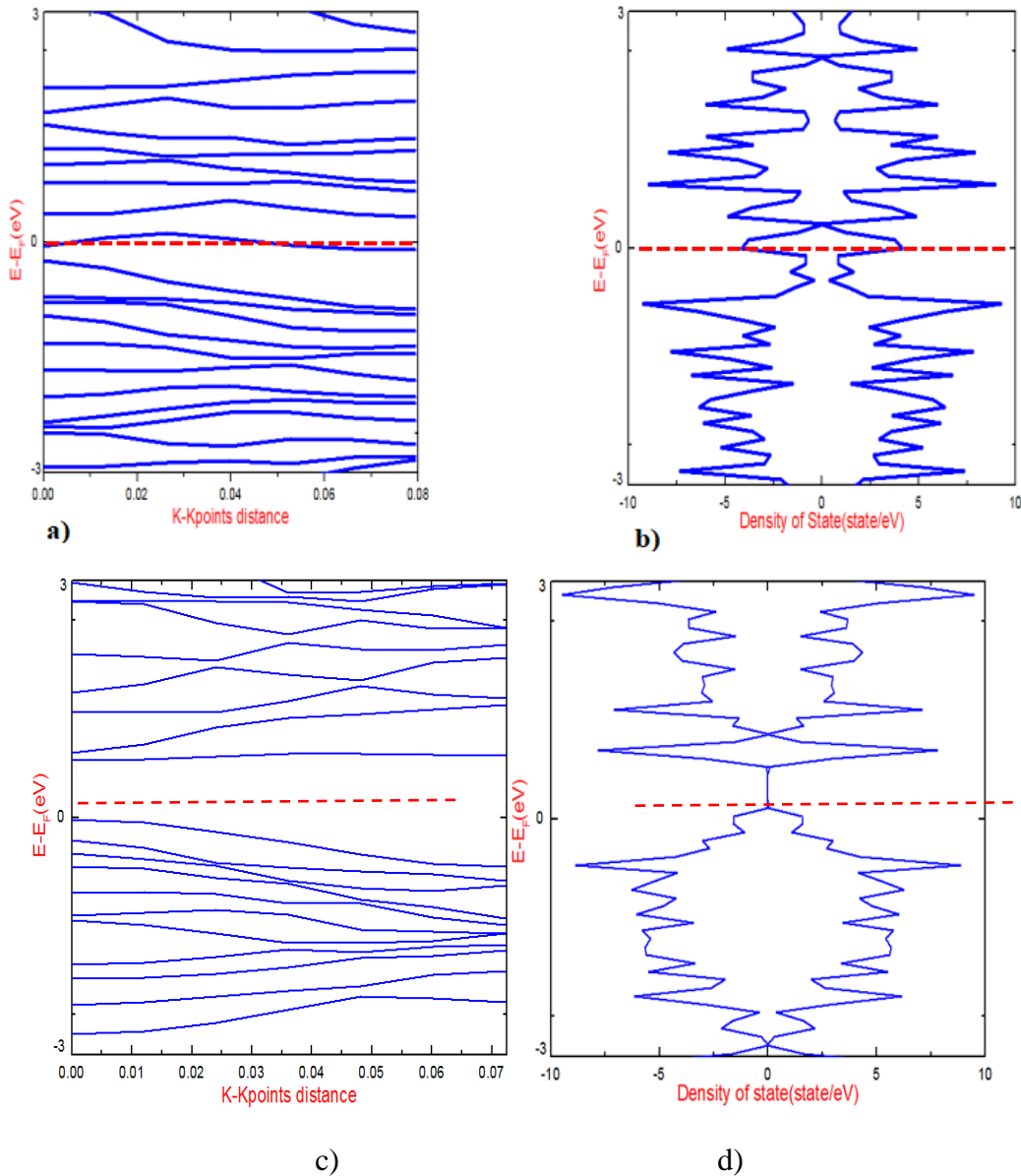


Figure 4. Band structures and the density of state of adsorption configurations of 1F-GeNR.out (a, b), and 2F-GeNR.out (c, d).

Figure 5 shows the part density of state of the adsorption configurations of 1F-GeNR.bridge (a), 2F-GeNR.bridge(b), 1F-GeNR.out(c), and 2F-GeNR.out(d) for each element Ge and F. From the graphs of the part density of states (PDOS) in fig 5, we can see that the distribution of PDOS of Ge_S is mainly in low energy region, while that of PDOS of Ge_P is mainly in the region near the Fermi level and high energy conduction region. The state density of F_S has a negligible contribution over the entire energy range, while the state density of F_P is only significant in the very low energy region below the Fermi level in both two adsorption configurations of 1F-GeNR and 2F-GeNR. We also see that lines of F atom overlap on lines of Ge atom in the graph of

PDOS, this again shows both four adsorption configurations are chemical adsorptions. All four adsorption configurations and primary germanene are non-magnetic, these can be observed from the symmetry of state density of all configurations.

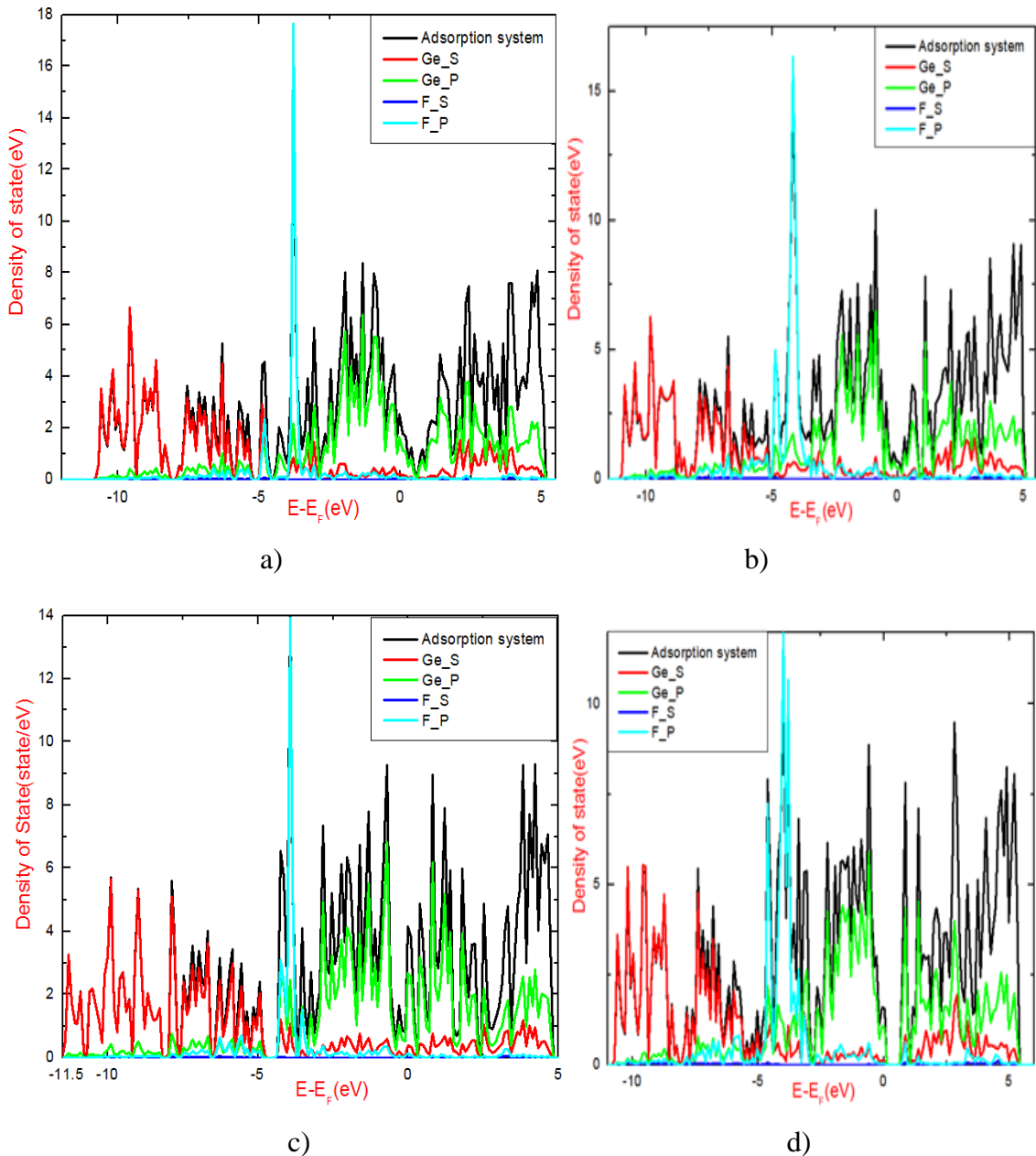


Figure 5. PDOS of every element in the adsorption configuration of 1F-GeNR.bridge (a), 2F-GeNR.bridge (b), 1F-GeNR.out (c), and 2F-GeNR.out (d).

6. The charge distribution

Figures 6, and 7 show the charge distribution in four configurations of 1F-GeNR.bridge, 1F-GeNR.out (a), and 2F-GeNR.bridge, 2F-GeNR.out (b).

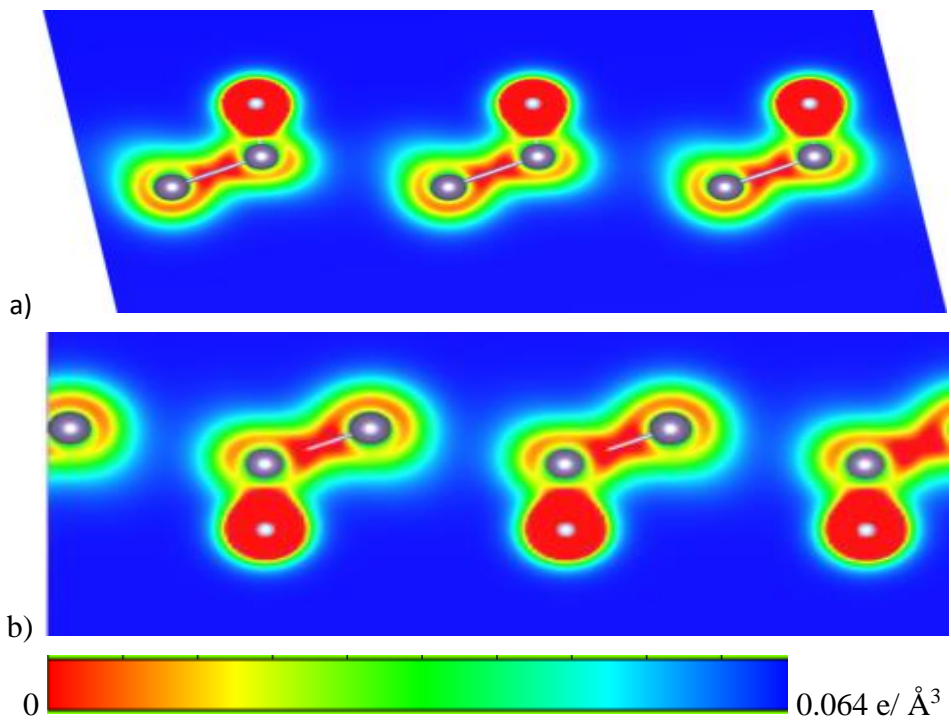


Figure 6. The charge distribution of the adsorption configurations of 1F-GeNR.bridge(a), 1F-GeNR.out (b).

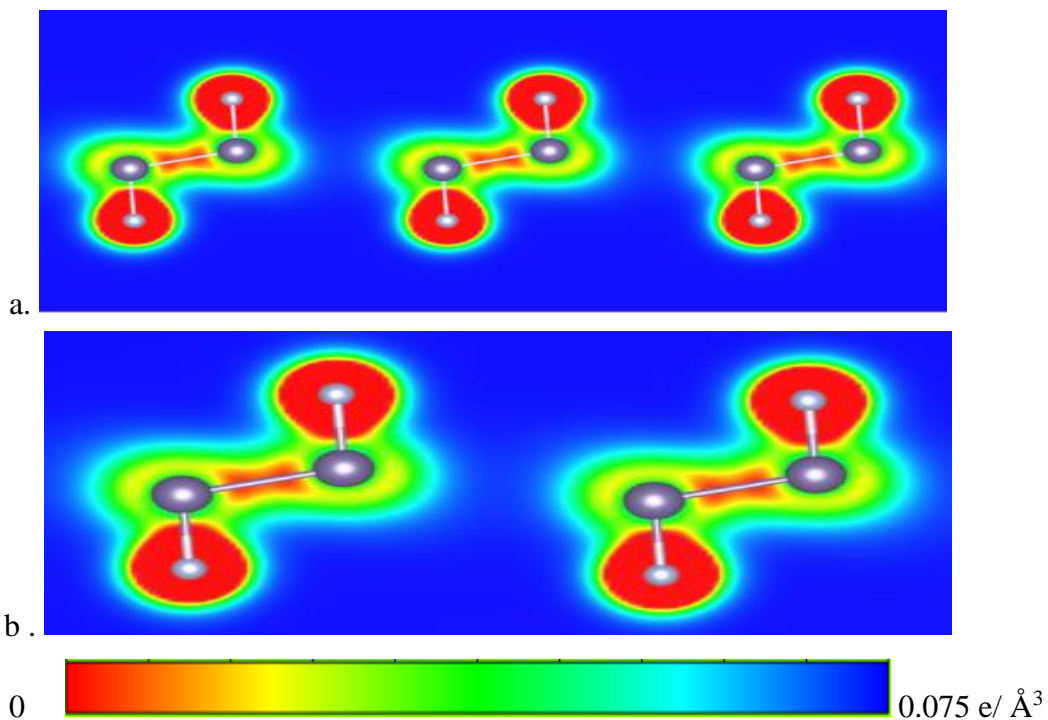


Figure 7. The charge distribution of the adsorption configurations of 2F-GeNR.bridge (a), and 2F-GeNR.out (b).

It is clear that electrons is pulled towards the F atom due to the larger electronegativity of F atoms (3.98) comparable to that of Ge atoms (2.01). The charge distribution of two strings of Ge atoms in the substrates is slightly different because the adsorption system of 2F-GeNR is symmetrically larger than that with two F atoms on two sides of the substrate. We can see in all adsorption configurations in fig 6, 7 that the space region between Ge-Ge atoms has a lighter red, yellow is dominant, which shows that the charge density is reduced in the substrate, while the space region around F atoms has a dark red color, which shows the charge density is increased around F atoms.

7. Conclusion

In conclusion, we studied the structural and electronic properties of adsorption systems of 1F-GeNR.bridge, 1F-GeNR.out, 2F-GeNR.bridge, and 2F-GeNR.out. Findings show the adsorption configuration of 1F-GeNR.bridge has no band structure, while other configurations are semimetals with band gap from 0.175eV to 0.67eV; both four adsorption configurations and pristine germanene are chemisorptions and non-magnetic. The investigation of the charge distribution in all four adsorption configurations shows that a charge transfer from the Ge atom to the F atom exists. Findings show that we can control the bandgap of germanene nanoribbon by changing the number of F atoms in the adsorbent system. This is very important in electronic applications.

References

- A. Dimoulas (2015). Silicene and germanene: Silicon and germanium in the “flatland”, *Microelectronic engineering*, 131, 68-78. <https://doi.org/10.1016/j.mee.2014.08.013>.
- A.H. Bayani, D. Dideban, N. Moezi (2016). Hydrogen sensitive field-effect transistor based on germanene nanoribbon and optical properties of hydrogenated germanene. *Journal of Computational Electronics*, 15, 381-388. <https://doi.org/10.1007/s10825-016-0797-2>.
- D. Chimene, D. L. Alge, A. K. Gaharwar (2015). Two-Dimensional Nanomaterials for Biomedical Applications: Emerging Trends and Future Prospects, *Adv Mater*, 27, 7261-84. <https://doi.org/10.1002/adma.201502422>.
- E. C. Anot, A. B. Hernández, M. Castro, G. H. Coccoletzi (2013). Density Functional Theory Studies of the Structural and Electronic Properties of Germanium Nanosheets. *Journal of Computational and Theoretical Nanoscience*, 10, 2264-2268. <https://doi.org/10.1166/jctn.2013.3196>.
- E.M. Abhinav, D.V. Chary (2014). Strain-induced on germanene monolayer 6nm short channel FET from first-principle study in International Conference on Circuits, Communication, Control and Computing. IEEE. 10.1109/CIMCA.2014.7057743.27

- H. Oughaddou, S. Sawaya, J. Goniakowski, B. Aufray, G. Le Lay, J. M. Gay, G. Trégliá, J. P. Bibérian, N. Barrett, C. Guillot, A. Mayne (2000). Ge/Ag (111) semiconductor-on-metal growth: Formation of an Ag₂Ge surface alloy, *Physical Review B*, 62, 16653. <https://doi.org/10.1103/PhysRevB.62.16653.26>
- H.J. Monkhorst, J.D. Pack (1976). Special points for Brillouin-zone integrations, *Phys.Rev. B* 13, 5188-5192. doi:10.1103/physrevb.13.5188.
<https://doi.org/10.1002/adma.201400909>.
<https://doi.org/10.1002/sml.201402041>.
<https://doi.org/10.1021/acs.nanolett.5b00085>.
- J.P. Perdew, K. Burke, M. Ernzerhof (1996). Generalized gradient approximation made simple, *Phys. Rev. Lett.* 77 (1996) 3865. doi:10.1103/physrevlett.77.3865
- Kresse, G. (1996). Efficient iterative schemes for ab initio total-energy calculations using a plane-wave basis set. *Phys.Rev.B* 54(16), 11169–11186. doi:10.1103/physrevb.54.11169
- L. Li, S. Z. Lu, J. Pan, Z. Qin, Y. Q. Wang, Y. Wang, G. Y. Cao, S. Du, H. J. Gao (2014). Buckled germanene formation on Pt (111), *Advanced Materials*, 26, 4820-4824.
- L. Matthes, F. Bechstedt (2014). Influence of edge and field effects on topological states of germanene nanoribbons from self-consistent calculations, *Physical Review B*, 90, 165431. <https://doi.org/10.1103/PhysRevB.90.165431>.
- M. Derivaz, D. Dentel, R. Stephan, M.C. Hanf, A. Mehdaoui, P. Sonnet, C. Pirri (2015). Continuous germanene layer on Al (111), *Nano letters*, 15, 2510-2516.
- M. E. Dávila, L. Xian, S. Cahangirov, A. Rubio, G. Le Lay (2014). Germanene: a novel two-dimensional germanium allotrope akin to graphene and silicene, *New Journal of Physics*, 16, 095002. <https://doi.org/10.1088/1367-2630/16/9/095002>.
- P. Bampoulis, L. Zhang, A. Safaei, R. van Gastel, B. Poelsema, H. J. W. Zandvliet (2014). Germanene termination of Ge₂Pt crystals on Ge (110), *Journal of physics: Condensed matter*, 26, 442001. <https://doi.org/10.1088/0953-8984/26/44/442001>.
- P. Rubio-Pereda, N. Takeuchi (2015). Adsorption of Organic Molecules on the Hydrogenated Germanene: A DFT Study, *the Journal of Physical Chemistry C*, 119, 27995-28004. <https://doi.org/10.1021/acs.jpcc.5b08370>. 28
- P.E. Blochl (1994). Projector augmented-wave method, *Phys. Rev. B* 50, 17953. <https://doi.org/10.1103/PhysRevB.50.17953>
- Q. Pang, L. Li, D. L. Gao, R. P. Chai, C. L. Zhang, Y. L. Song (2017). Tuning the electronic and magnetic properties of germanene by surface adsorption of small nitrogen-based molecules, *Physica E: Lowdimensional Systems and Nanostructures*, 88, 237-242. <https://doi.org/10.1016/j.physe.2017.01.018>.
- Q. Pang, Y. Zhang, J. M. Zhang, K. W. Xu (2011). Functionalization of low-dimensional honeycomb germanium with 3d transition-metal atoms, *Computational Materials Science*, 50 (2011) 1717-1724. <https://doi.org/10.1016/j.commatsci.2011.01.002>.
- S. Balendhran, S. Walia, H. Nili, S. Sriram, M. Bhaskaran (2015). Elemental analogues of graphene:silicene, germanene, stanene, and phosphorene, *small*, 11, 640-652.
- S. Cahangirov, M. Topsakal, E. Aktürk, H. Şahin, S. Ciraci (2009). Two-and one-dimensional honeycomb structures of silicon and germanium, *Physical review letters*, 102, 236804. <https://doi.org/10.1103/PhysRevLett.102.236804>.

- S. Cahangirov, M. Topsakal, S. Ciraci (2010). Armchair nanoribbons of silicon and germanium honeycomb structures, *Physical Review B*, 81, 195120. <https://doi.org/10.1103/PhysRevB.81.195120>.
- S. Dong, C. Q. Chen (2015). Stability, elastic properties, and electronic structure of germanane nanoribbons, *J Phys Condens Matter*, 27, 245303. <https://doi.org/10.1088/0953-8984/27/24/245303>.
- S. Jiang, M. Q. Arguilla, N. D. Cultrara, J. E. Goldberger (2014). Covalently-controlled properties by design in group IV graphane analogues, *Accounts of chemical research*, 48, 144-151. <https://doi.org/10.1021/ar500296e>.
- W. Xia, W. Hu, Z. Li, J. Yang (2014). A first-principles study of gas adsorption on germanene, *Physical Chemistry Chemical Physics*, 16, 22495-22498. <https://doi.org/10.1039/C4CP03292F>.
- Y. P. Wang, W. X. Ji, C. W. Zhang, S. S. Li, F. Li, P. Li, M. J. Ren, X. L. Chen, M. Yuan, P. J. Wang (2016). Enhanced band gap opening in germanene by organic molecule adsorption, *Materials Chemistry and Physics*, 173, 379-384. <https://doi.org/10.1016/j.matchemphys.2016.02.026>.